

# Performance Characteristics of the 3-DISS Surface Contamination Monitor

**Michael J. Schierman, Charles P. Farr, Neil Wrubel, and Kenneth R. Baker**

**Environmental Restoration Group, Inc. Key Words: contamination monitor**

## **Abstract**

The Three-Dimensional Indoor Survey System (3-DISS) consists of a fan laser positioning system coupled to a multiple detector array or single hand-held radiation detector to accurately record radiation emissions and corresponding x, y, z coordinates. The performance characteristics of the 3-DISS have been evaluated when using alpha and beta detectors. The integrated counts and associated coordinates are recorded at the end of each counting interval and downloaded into ArcView GIS for data processing and presentation. Commercially available digital ratemeter/scalers with RS-232 output capability were modified to provide scaler outputs at user specified multiples of one second intervals. Because of the short counting time, small sample statistics were used to model the expected output. The statistically derived frequency distributions of counts per counting interval were found to agree well with actual results. The variance of the calculated count rates may be reduced during data processing by nearest-neighbor-averaging techniques, thereby reducing the occurrence of false positives and false negatives. This also minimizes the spatial distortion of the contaminant distribution on a surface when compared to traditional survey methods. The statistical model of the 3-DISS was used to provide the minimum detectable concentration as a function of background count rate, counting interval, number of nearest neighbors, and the detector detection efficiency.

## **1. Introduction**

The Three Dimensional Indoor Survey System (3-DISS) consists of Ludlum Model 2360 ratemeters/scalers coupled to radiation detectors. The three different configurations include a hand-held unit, a floor monitor, and a wall scanner. The firmware in the Ludlum 2360 digital ratemeters/scalers was modified to provide a scaler count output in multiples of 1-second intervals. When scanning, the integrated counts and associated x, y, and z coordinates are automatically recorded at the end of each

integrating period. This integration period will be referred hereafter as the counting interval. When in the static count mode, a pre-selected count time is used and the data and associated coordinates are automatically recorded at the end of the count time.

The detectors used for the hand-held units are either gas proportional detectors (Ludlum 43-68) or dual phosphor scintillation probes (Ludlum 43-93). The floor monitor/wall scanner consists of a single Ludlum 43-134 gas proportional detector. The detector is 115 cm long and 14.4 cm wide, and has eight 100-cm<sup>2</sup> active zones with no dead space between zones. A detector holder was also designed for the Ludlum 43-93 detectors where the detectors are staggered and overlapped so 100 percent of the area is scanned. The 6.9 cm by 14.5 cm detectors are aligned so the width of the eight-detector array is 116 cm.

The Ludlum Model 2360 ratemeter/scaler has two channels for counting: a low amplitude pulse channel (typically 4 mV-40 mV) and a high amplitude channel which counts every pulse above approximately 150 mV. Beta particles normally have a lower energy than alpha particles and thus the high voltage can be adjusted so the beta particles are detected in the low voltage channel and the alpha particles in the high voltage channel. Note there is a small voltage region where the pulses are lost and thus the efficiency of the detectors is diminished. There is also cross-talk between the channels. In particular, approximately 10 percent of the alpha particles will be registered as beta particles. This can be explained by alpha particle energy degradation arising from scattering with the source, molecules of air, or detector window material.

This paper models the performance characteristics of the 3-DISS, considering such parameters as counting interval, detector efficiency, source strength, and background count rates. It will be shown that the detection sensitivity can be improved significantly by processing the data using nearest-neighbor averaging techniques. Improvements relative to the use of conventional digital ratemeter outputs will be discussed.

Only uniformly contaminated or natural background levels of contamination are considered in the models. Detection probabilities for "hot spots" have been studied but are beyond the scope of this paper.

Emphasis is placed on beta surveys since the higher beta background count rates render interpretation of the beta data problematic.

## 2. Statistics

The number of detected counts in most practical counting intervals while scanning for particle emissions will be fewer than 30 and thus can be represented by a Poisson distribution. This discrete probability distribution can be calculated using the equation,

$$P(x) = \lambda^x e^{-\lambda} / x!$$

Where  $x = 0, 1, 2, \dots$  and  $\lambda = \text{mean}$ . The variance  $\sigma^2$  is equal to the mean. For high count rates where the number of counts per counting interval is large, the Poisson distribution may be approximated by a normal distribution.

## 3. Detector Efficiencies

Detector efficiencies have been measured using plated NIST traceable sources. For scanning smooth surfaces, a scanning distance of 0.25 inch is assumed where alpha efficiencies of approximately 0.08-0.18 are expected. For beta emitters, efficiencies in the range of 0.10-0.20 are anticipated, based on  $4\pi$  emission rates of the source. For most of the illustrations in this paper, alpha and beta efficiencies of 0.10 and 0.15 have been used, respectively.

## 4. Background

Typical instrument background alpha and beta count rates for a 100-cm<sup>2</sup> gas proportional detector of 4 cpm and 250 cpm, respectively, have been used in most of the illustrations in this paper. The Poisson probability distributions of obtaining exactly N counts in a counting interval for the alpha and beta background count rates are shown in Figures 4-1 and 4-2, respectively, for 1 second and 3 second counting intervals.

Since radiation detectors do not differentiate between counts from background and counts from a source, a 100-cm<sup>2</sup> alpha background count rate of 4 cpm will, on the average, respond like a surface contaminated at 40 dpm/100 cm<sup>2</sup> (4 cpm/0.10 cpm/dpm). However, because of the short count times, a

Poisson distribution will be observed. If one event is detected during the one second interval, it will be recorded as 600 dpm/100 cm<sup>2</sup> (1\*60 cpm/0.10 cpm/dpm). If one count is recorded in a 3 second interval, it will be recorded as 200 dpm/100 cm<sup>2</sup> (1\*20 cpm/0.10 cpm/dpm), etc. Fig. 4-1 shows that most of the counting intervals will have no counts. However, for both counting intervals, the average count rate is equivalent to a count rate of 4 cpm, or a reported count rate of 40 dpm/100 cm<sup>2</sup>.

Fig. 4-2 shows the calculations for the beta background, where the background is assumed at 250 cpm for a 100-cm<sup>2</sup> detector having an efficiency of 0.15 cpm/dpm. An average background count rate of 250 cpm will result in the detector reporting a mean of 1667 dpm/100 cm<sup>2</sup> (250/0.15). As can be seen in Fig. 4-2, a distribution of numbers will be recorded with the mean in each case being 1667 dpm/100 cm<sup>2</sup>. Again, the variance or spread of the numbers is less for the longer count interval.

## **5. Scanning a Uniformly Contaminated Area**

This section includes an analysis of the performance characteristics for a 100-cm<sup>2</sup> detector while scanning a surface uniformly contaminated at 1000 dpm/100 cm<sup>2</sup>. Counting intervals of 1 and 3 seconds have been considered along with a detection efficiency of 0.10 cpm/dpm for alpha and 0.15 for beta.

### **5.1 Alpha Scanning**

Fig. 5-1 and Fig. 5-2 show the calculated Poisson distributions of counts per counting interval for 1 second and 3 second counting intervals. The source counts plus background counts per counting interval is shown as one histogram while the background counts per counting interval is shown as another histogram. The Poisson distributions have been multiplied by the average count/counting interval, resulting in the sum of the heights of each histogram (area under the curve) being equal to the average counts/counting interval.

A decision level may be selected from the data used to create these histograms, to take an action, such as declaring the area contaminated. No appropriate decision level is evident in Fig. 5-1, at which an area can be declared contaminated at 1,000 dpm/100 cm<sup>2</sup> without an unacceptably large error rate of calling events arising from background as contaminated above the 1,000 dpm/100 cm<sup>2</sup> level.

The results for the 3 second counting interval are shown in Fig. 5-2. Increasing the counting interval significantly reduces the number of counting intervals with zero counts when the source is present. If a decision level of 500 dpm/100 cm<sup>2</sup> or more is selected as representative of what would be expected from a surface contaminated at 1000 dpm/100 cm<sup>2</sup>, a false positive probability of  $1 - 0.819 = 0.164$ , or 0.164 is expected. Using the same decision level, the data for the case where the source is present in addition to background indicates a false negative value of 0.035. These error rates for the 3 second interval are considered acceptable for most applications.

## **5.2 Beta Scanning**

A similar analysis for beta scanning shows that the 1 second counting interval produced high error rates for any decision level chosen. The 3 second counting interval beta scanning performance data for a uniformly contaminated surface, contaminated at 1000 dpm/100 cm<sup>2</sup>, a background count rate of 250 cpm/100 cm<sup>2</sup>, and a detector efficiency of 0.15 cpm/dpm are shown in Fig. 5-3. The overlap for the 3 second counting interval is much less than for the 1 second interval, but there is no decision level at which both the false positive and false negative errors are less than 15 percent. Therefore, unless the background is considerably less or the source is stronger, beta scanning with a 3 second or less counting interval does not provide definitive data at a reasonably low tolerance for error. In Section 6, we use a nearest-neighbor-averaging technique on this data set to illustrate the benefits of processing the data.

## **6.0 Data Processing Using Nearest Neighbor Averaging Techniques**

The sections above indicate that the performance of the system can be predicted accurately and decision levels can be determined with known levels of confidence. However, for beta scanning, a 3 second or less counting interval results in unacceptable error rates for the assumed conditions, unless the variance of the data set can be reduced. The benefits and method for reducing the variance is presented in the following sections.

## 6.1 Benefits from Data Processing

Low count-rate scanning measurements have always been subject to high levels of variability. Older ratemeters employed RC circuits to reduce the fluctuations. Modern digital ratemeters use averaging techniques to produce similar results. At low count rates, it takes the Ludlum 2360 ratemeter 7 seconds to record an initial 10 to a final 90 percent of the maximum reading. When scanning under these conditions, the instantaneous reading usually is not representative of the conditions beneath the detector.

The 3-DISS system employs modified Ludlum 2360 ratemeters where a scaler output (rather than a ratemeter output) is received at prescribed time intervals. Time intervals of one to three seconds when using typical scanning speeds allow data to be recorded in the immediate vicinity of the area on which it is collected. The statistical variation is reduced through a data processing technique, called nearest neighbor averaging. If done properly and coordinated with the scanning speed, the statistical variation can be reduced without introducing the spatial distortion described above.

## 6.2 Nearest Neighbor Averaging

Actual counts per interval are recorded for a counting interval and ArcView GIS is used to “smooth” the data using nearest neighbor averaging techniques. Each datum is replaced by a new number which is the average of it and its nearest neighbors. This new data set represents a smoothing of the data similar to that obtained from a ratemeter. However, it differs from a ratemeter, because the spatial misrepresentations discussed above are minimized.

### 6.2.1 Statistical Basis

Elementary sampling theory (Hoel, 1962) for normal distributions states:  
Suppose that all possible samples of size  $n$  are drawn with replacement from a finite population of size  $n_p > n$ . If we denote the mean and standard deviation of the sampling distribution of means by  $\mu_{\bar{x}}$  and  $\sigma_{\bar{x}}$  and the population mean and standard deviation by  $\mu$  and  $\sigma$  respectively, then the sample mean will be normally distributed with  $\mu_{\bar{x}} = \mu$  and  $\sigma_{\bar{x}} = \sigma / \sqrt{n}$ .

Each nearest neighbor data set is made up of means of samples taken from the original population ( $N=0$ ) with replacement. Thus the sampling distribution of the mean will have a mean approximately equal to the mean of the original data set ( $N=0$ ). Also the standard deviation of the sampling distribution will be approximately equal to the standard deviation of the original data set divided by the square root of the number corresponding to the sample size. In our case, the sample size is  $N+1$ .

A second theorem, the central limit theorem, states that even for non-normal distributions of  $x$ , the sampling distribution of means converge to a normal distribution as the number of samples goes to infinity. This is particularly important when applying nearest neighbor averaging techniques to alpha data since the distribution is not normal for background or slightly contaminated areas. However, normal statistics may be applied to distributions after nearest neighbor averaging if the number of data points is large. Since scans at low speeds result in high data density, the number of data points in an area is usually large.

### ***6.2.2 Test of Theory***

In scanning an area at 5 cm/second, recording data at 3-second intervals produces data at a density equivalent to grid nodes of approximately 15-cm by 15-cm, or approximately 45 data points per square meter. Therefore nearest neighbor averaging of data over any uniformly contaminated area of significant size will result in a large data set whose mean and standard deviation should follow theoretical predictions.

As a test of the central limit theorem for our application, 500 whole numbers within the range 0-3 were generated and placed in a MS Excel column using a random number generator. The unprocessed data in this first column showed a distribution that was approximately rectangular with approximately the same number of 0, 1, 2, and 3 values. Two additional columns were generated of nearest neighbor averages of the first column numbers for  $N=2$  and  $N=4$ . Plots of the frequency distributions showed that both the  $N=2$  and  $N=4$  columns were normally distributed with means of all columns approximately

equal. The standard deviations followed the relationship,  $\sigma_{\bar{x}} = \sigma / \sqrt{N + 1}$ , where N is the number of nearest neighbors and  $\sigma$  is the standard deviation of the unprocessed data.

A simple test of the statistics of averaging was done by placing a Ludlum 43-93 alpha/beta detector in an uncontaminated location and recording approximately 275 alpha and beta counts in 2 second counting intervals. A statistical summary of the data is shown in the top half of Table 6-1 under the column heading N=0. MS Excel was used to average each record with the N nearest neighbors preceding and following it in time. A new data set was created to include these averages. The columns under N=2 contain the statistics for this new set of data. For N=4, five records were averaged, two before and two after. The three records before and after each record were used for N=6. The measured standard deviation indicated in Table 6-1 clearly becomes smaller as N increases. The fifth line (Theory) in Table 6-1 gives the calculated mean and standard deviation calculated by dividing the standard deviation of the untransformed population distribution (N=0) by  $\sqrt{N + 1}$ . As can be seen from the table, the theoretical standard deviation agrees well with the calculated standard deviation.

### ***6.2.3 Interpretation of Data***

It is always preferable to the novice statistician to work with data that are normally distributed. Theory, as supported by actual data, presented in prior sections has shown that unprocessed data will have a Poisson distribution. As the counts per counting interval increase, the Poisson distribution may be represented by a normal distribution. For data sets made up of nearest neighbor averages, the distribution will be normal or become normal as the number of averages within the data set become very large, depending on how close to normal the unprocessed data distribution is. Once the distribution has been established, the properties of the distribution may be used to establish decision levels related to exceeding derived concentration guideline levels (DCGL) or other goals.

The decision level is a record above which some action should be taken. Normally this is a level that exceeds the DCGL but it may also be an ALARA level at which some action, such as further

decontamination is attempted. Multiple action levels may be established. In all cases, the detector background and efficiency is measured and the detector performance modeled.

The 3 second counting interval for beta scanning can be approximated by a normal distribution, as shown in Fig. 6-1, even at background levels without nearest neighbor averaging. As indicated in Section 5, interpretation of the raw data can be problematic because of high statistical variations. To predict the effect of performing a nearest neighbor averaging technique, a theoretical transformation was applied to the frequency distributions in Fig. 5-3. The new distribution will have the same mean but the standard deviation will be reduced by a factor of  $1/\sqrt{N+1}$ . The Poisson distributions in Fig. 5-3 have been approximated by a normal distribution. Fig. 6-1 shows the background distribution from Fig. 5-3, along with the product of the mean times the normalized normal distribution function. Obviously, a good fit exists for this test case and thus distributions obtained from the nearest neighbor averaging techniques can be calculated using the normal distribution function.

Fig. 6-2 and Fig. 6-3 show the results after applying the nearest neighbor averaging technique for  $N=2$  and  $N=4$  to the background distribution and the background plus 1000 dpm/100 cm<sup>2</sup> distribution. In this case, nearest neighbor averaging renders the data into a form that is more easily interpreted when comparing these figures to Fig. 5-3. For example, if the goal was to establish a decision level above which areas contaminated at 1000 dpm/100 cm<sup>2</sup> above background were identified as contaminated and background levels were labeled as background, a decision level of 2001 dpm/100 cm<sup>2</sup> might be chosen. In this case, a false positive is a count indicating an area is contaminated at 1000 dpm/100 cm<sup>2</sup> above background when it is actually at a background level of 250 cpm. A false negative is an event perceived as background when it actually arises from a contaminated area of 1000 dpm/100 cm<sup>2</sup> above background. Using that decision level, an assessment of the data shows that the unprocessed data (Fig. 5-3) would result in a false positive probability of 0.197 and a false negative probability of 0.157. Performing nearest neighbor averaging clearly reduces the false negative and false positive probabilities to acceptable levels, as shown in Table 6-2.

This exercise illustrates that the system will distinguish areas with contamination at 1000 dpm/100 cm<sup>2</sup> (or higher) above background provided the scanning speed is such that the detector is over the area for 3 seconds or more. Since the gas proportional detector is 7 cm by 14.4 cm and the scanning direction is parallel to the short side, the minimum size hot spot, assuming a scanning speed of 4 cm/s is 14.4 cm x (7 + 12) cm = 274 cm<sup>2</sup>. This is an acceptably small area considering that contamination is normally allowed to be averaged over 1 m<sup>2</sup> (e.g., U.S. NRC Reg. Guide 1.86).

## 7. Minimum Detectable Concentration

The minimum detectable concentration (MDC), expressed in dpm/100 cm<sup>2</sup>, is the level that will be falsely considered as background only five percent of the time. Note in this case, the MDC will include the contribution from background and the “Net MDC” will be obtained by subtracting the background. In statistical terms, the Critical Level ( $L_c$ ) is defined as the number of counts per counting interval below which a count is considered a background event. For this exercise, we have placed the Critical Level at a point where there is a five percent probability ( $\alpha = 0.05$ ) of mistakenly interpreting a background count as exceeding background. This and the two frequency distributions are shown in Fig. 7-1. The variances ( $\sigma^2$ ) for the frequency distributions are equal to the means.

Fig. 7-1 will be used to derive the MDC using normal statistics. As demonstrated in Section 6, the associated frequency distributions could be described by normal statistics and the application of nearest neighbor averaging reduced the variance of the distribution in a predictable manner. From the figure,

$$L_c = B + k\sqrt{B}$$

$$L_c = MDC - k\sqrt{MDC}$$

Where  $k = 1.645\sqrt{N + 1}$  corresponding to  $\alpha = \beta = 0.05$  and  $N$  is the number of nearest neighbors averaged when transformed data are used. The terms  $\sqrt{B}$  and  $\sqrt{MDC}$  are the standard deviations of the two frequency distributions. These two equations can be combined so that

$$B + k\sqrt{B} = MDC - k\sqrt{MDC}$$

Letting  $x^2 = \text{MDC}$ , the equation can be written as:

$$x^2 - kx - (B + k\sqrt{B}) = 0$$

Solving the quadratic equation and choosing the positive quantity yields

$$\text{MDC} = \left( \frac{k + \sqrt{k^2 + 4L_c}}{2} \right)^2$$

Net MDC tables can be easily generated for a particular detector as a function of counting interval, detector efficiency, and detector background. If nearest neighbor averaging is used, the number of neighbors averaged is also a parameter. Table 7-1 consists of calculations made for the beta detector using a 3 second counting interval. The Net MDC increases as background counts increase. It decreases with increases in detector efficiency and the number of nearest neighbors used in the averaging. For a beta detecting efficiency of 0.15 and background count rate of 250 cpm, the Net MDC of the detector was calculated at 1912, 1016, 766, and 638 dpm/100 cm<sup>2</sup> when averaged with its N nearest neighbors of 0, 2, 4, and 6, respectively.

## 8. Conclusion

This work supports a new scanning system designed to present an accurate high density data map of alpha and beta surface contamination. Short counting intervals were used to avoid the spatial distortion of the contamination on surfaces obtained using conventional ratemeters. The short counting interval, however, results in high variability of the counts/counting interval which makes interpretation of the raw data difficult. This problem is mitigated through application of a nearest neighbor averaging technique, which reduces the variance of the data and has the additional advantage of allowing the use of normal statistics to describe the distributions.

## 9. References

Hoel PG, 1962. Introduction to Mathematical Statistics, John Wiley & Sons, Inc., New York, New York, 1962.

Table 6-1 Statistics from Averaging Each Datum with the N Nearest Neighbors

Background								
Statistic	N=0		N=2		N=4		N=6	
	$\alpha$	$\beta$	$\alpha$	$\beta$	$\alpha$	$\beta$	$\alpha$	$\beta$
Max	3	9	1.00	6.33	0.80	5.80	0.71	5.43
Min	0	0	0.00	1	0.00	1.40	0.00	1.57
Avg	0.11	3.26	0.11	3.28	0.11	3.29	0.11	3.29
Std Dev	0.36	1.73	0.19	1.00	0.15	0.79	0.13	0.69
Theory Std Dev			0.21	1.00	0.16	0.77	0.14	0.65
Background Plus Source								
Statistic	N=0		N=2		N=4		N=6	
	$\alpha$	$\beta$	$\alpha$	$\beta$	$\alpha$	$\beta$	$\alpha$	$\beta$
Max	2	28	1.33	19.67	1.00	18.00	0.86	17.57
Min	0	6	0.00	10	0.00	11.20	0.00	11.71
Avg	0.18	14.91	0.18	14.89	0.18	14.87	0.18	14.86
Std Dev	0.44	3.34	0.27	2.09	0.21	1.38	0.18	1.11
Theory Std Dev			0.25	1.93	0.20	1.49	0.17	1.26

Table 6-2 Error Rates for 3-Second Interval Beta Scanning

Data Set	False Positive Probability <sup>a</sup>	False Negative Probability <sup>a</sup>
Unprocessed Data	0.13	0.14
Two Nearest Neighbors	0.023	0.032
Four Nearest Neighbors	0.0046	0.0081
Six Nearest Neighbors	0.00087	0.0021

Note:

a. Decision Level at 2001 dpm/100 cm<sup>2</sup>

Table 7-1 Net Beta Contamination MDC for a 3 Second Counting Interval (dpm/100 cm<sup>2</sup>)

N=6		Detector Efficiency									
Background	0.1	0.11	0.12	0.13	0.14	0.15	0.16	0.17	0.18	0.19	0.2
150	758	689	632	583	542	506	474	446	421	399	379
200	864	785	720	664	617	576	540	508	480	455	432
250	957	870	797	736	683	638	598	563	531	503	478
300	1041	946	867	800	743	694	650	612	578	548	520
N=4		Detector Efficiency									
Background	0.1	0.11	0.12	0.13	0.14	0.15	0.16	0.17	0.18	0.19	0.2
150	914	831	762	703	653	609	571	538	508	481	457
200	1039	944	866	799	742	693	649	611	577	547	519
250	1149	1044	957	884	820	766	718	676	638	605	574
300	1248	1134	1040	960	891	832	780	734	693	657	624
N=2		Detector Efficiency									
Background	0.1	0.11	0.12	0.13	0.14	0.15	0.16	0.17	0.18	0.19	0.2
150	1221	1110	1017	939	872	814	763	718	678	643	610
200	1382	1256	1151	1063	987	921	864	813	768	727	691
250	1524	1385	1270	1172	1088	1016	952	896	846	802	762
300	1652	1502	1376	1271	1180	1101	1032	972	918	869	826
N=0		Detector Efficiency									
Background	0.1	0.11	0.12	0.13	0.14	0.15	0.16	0.17	0.18	0.19	0.2
150	2343	2130	1953	1802	1674	1562	1465	1378	1302	1233	1172
200	2622	2384	2185	2017	1873	1748	1639	1542	1457	1380	1311
250	2868	2607	2390	2206	2048	1912	1792	1687	1593	1509	1434
300	3090	2809	2575	2377	2207	2060	1931	1817	1716	1626	1545

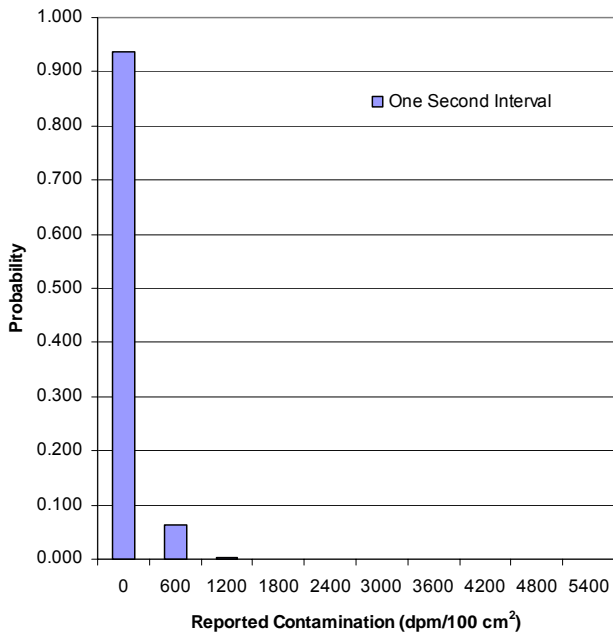


Fig. 4-1a Probability Distribution of Reported Surface Contamination from Alpha Background-1 Second Interval

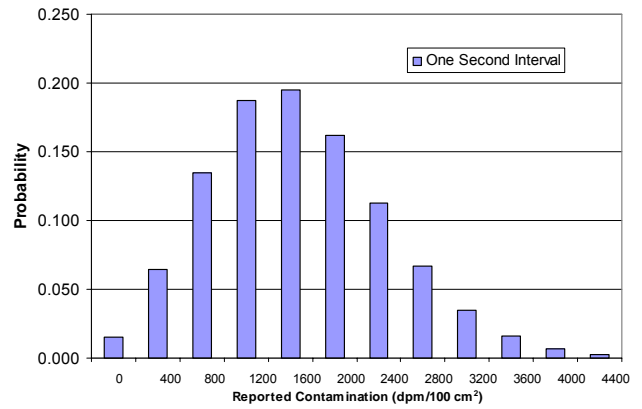


Fig. 4-2a Probability Distribution of Reported Surface Contamination from Beta Background-1 Second Interval

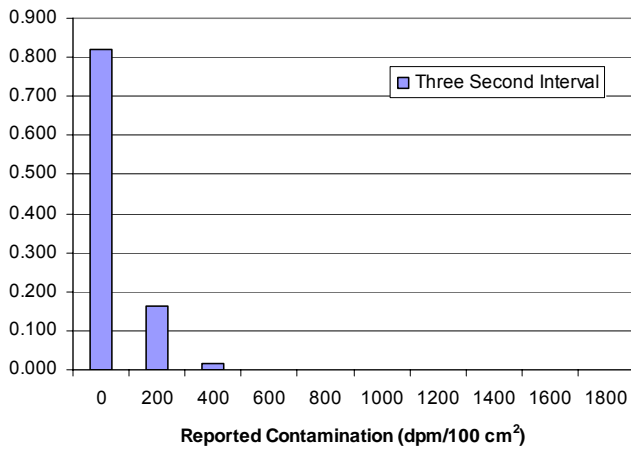


Fig. 4-1b Probability Distribution of Reported Surface Contamination from Alpha Background-3 Second Interval

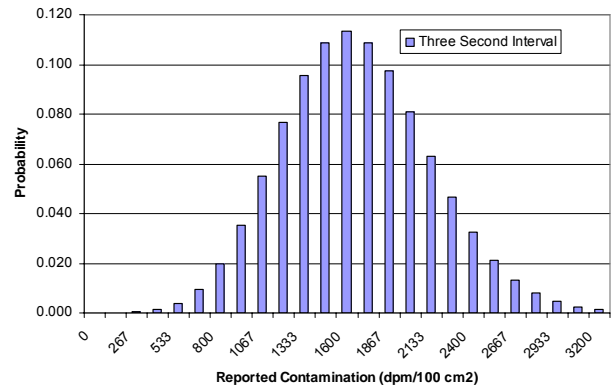


Fig. 4-2b Probability Distribution of Reported Surface Contamination from Beta Background-3 Second Interval

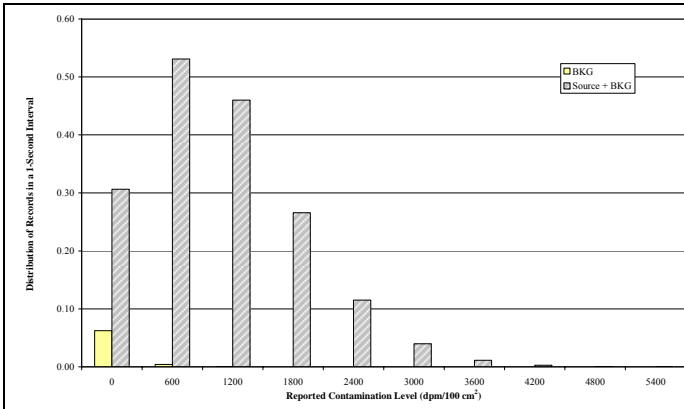


Fig. 5-1 Alpha Contamination Probability Distribution 1 Second Counting Interval

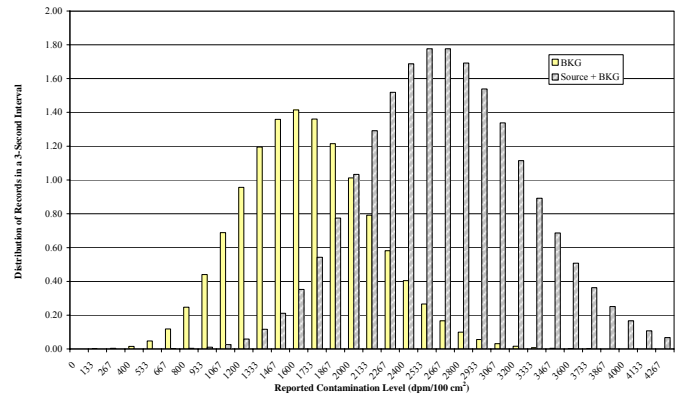


Fig. 5-3 Beta Contamination Probability Distribution for a 3 Second Counting Interval

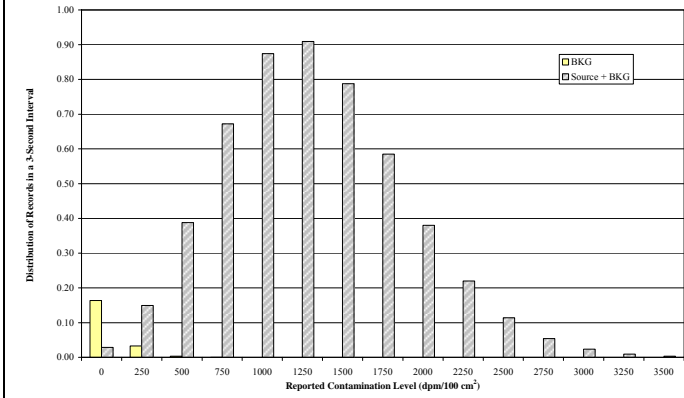


Fig. 5-2 Alpha Contamination Probability Distribution for a 3 Second Counting Interval

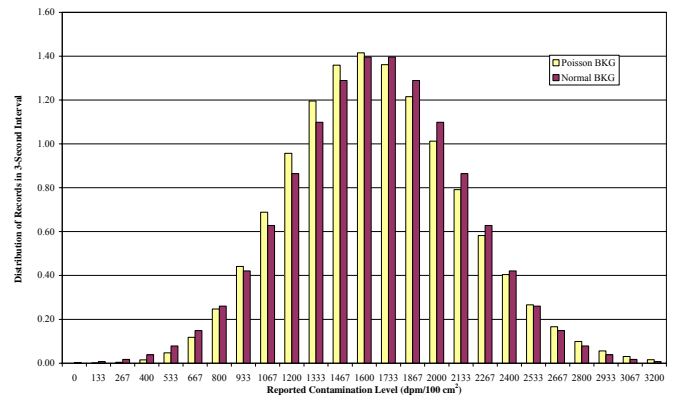


Fig. 6-1 Background Beta Probability Distributions, Poisson versus Normal

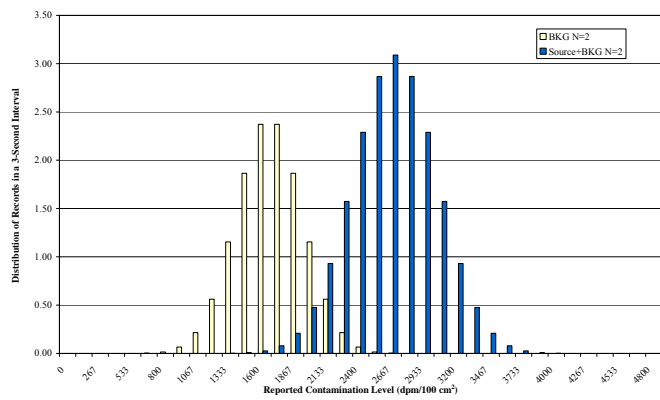


Fig. 6-2 Nearest Neighbor Averaged N=2 Beta Contamination Probability Distribution

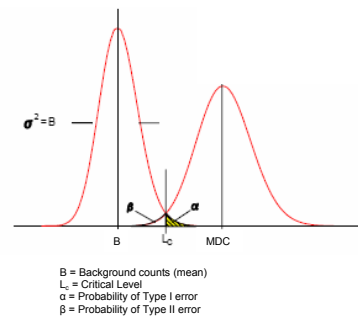


Fig. 7-1 Frequency Distributions for MDC Determination

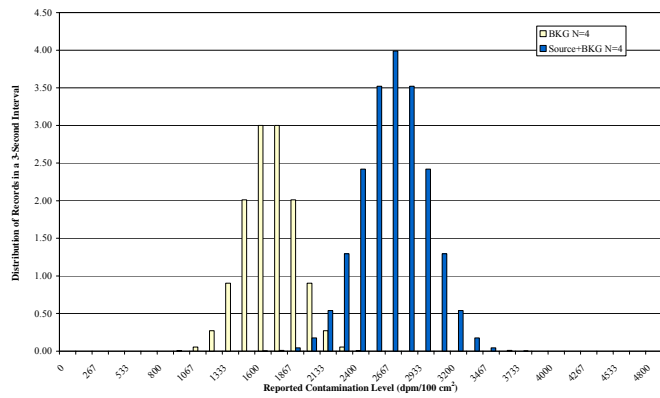


Fig. 6-3 Nearest Neighbor Averaged N=4 Beta Contamination Probability Distribution